RAGE Deficiency Improves Postinjury Sciatic Nerve Regeneration in Type 1 Diabetic Mice

Judyta K. Juranek,[1] Matthew S. Geddis,[1,2] Fei Song,[1] Jinghua Zhang,[1] Jose Garcia,[3] Rosa Rosario,[1] Shi Fang Yan,[1] Thomas H. Brannagan,[3] and Ann Marie Schmidt[1]

Peripheral neuropathy and insensate limbs and digits cause significant morbidity in diabetic individuals. Previous studies showed that deletion of the receptor for advanced end-glycation products (RAGE) in mice was protective in long-term diabetic neuropathy. Here, we tested the hypothesis that RAGE suppresses effective axonal regeneration in superimposed acute peripheral nerve injury attributable to tissue-damaging inflammatory responses. We report that deletion of RAGE, particularly in diabetic mice, resulted in significantly higher myelinated fiber densities and conduction velocities consequent to acute sciatic nerve crush compared with wild-type control animals. Consistent with key roles for RAGE-dependent inflammation, reconstitution of diabetic wild-type mice with RAGE-null versus wild-type bone marrow resulted in significantly improved axonal regeneration and restoration of function. Diabetic RAGE-null mice displayed higher numbers of invading macrophages in the nerve segments postcrush compared with wild-type animals, and these macrophages in diabetic RAGE-null mice displayed greater M2 polarization. In vitro, treatment of wild-type bone marrow–derived macrophages with advanced glycation end products (AGEs), which accumulate in diabetic nerve tissue, increased M1 and decreased M2 gene expression in a RAGE-dependent manner. Blockade of RAGE may be beneficial in the acute complications of diabetic neuropathy, at least in part, via upregulation of regeneration signals. ***Diabetes*** **62:931–943, 2013**

Diabetes leads to the development of multiple complications (1–3). Peripheral neuropathy affects 30–50% of all diabetic patients (4–6). Individuals with diabetes are more vulnerable to superimposed thermal and pressure injuries (7–10). Diabetic individuals exposed to either topical application of capsaicin or intracutaneous excision axotomy (punch skin biopsy) displayed a reduction in regenerative rate, even without evidence of neuropathy, and reduced axonal regenerative sprouting and blood vessel growth, respectively, compared with nondiabetic control subjects (11,12). Studies of diabetic animals reported a delay of axonal regeneration after acute sciatic nerve crush compared with nondiabetic mice (13). Evidence suggests that enhanced accumulation of advanced glycation end products (AGEs) may be an important contributing mechanism to the pathogenesis of diabetes complications (14,15). AGEs are a heterogeneous group of molecules that impact cellular properties and gene expression via specific receptors such as receptor for advanced end-glycation product (RAGE) (16–18). RAGE, a pattern recognition receptor, also interacts with multiple members of the proinflammatory S100/calgranulin family and with high-mobility group box 1 protein (HMGB1); both classes of molecules are implicated in inflammation and cellular migration (19,20). These non-AGE ligands may be released by dying cells, and evidence suggests that although RAGE is not intimately involved in innate immune responses, its upregulation and activation by these ligands contribute to sustained inflammation and suppression of repair (21,22).

These considerations prompted us to hypothesize that RAGE action in superimposed acute injury to the peripheral nerve, particularly in diabetes, attenuates neurite outgrowth and axonal regeneration via tissue-damaging inflammatory mechanisms. We subjected wild-type (WT) and homozygous RAGE-null mice to acute sciatic nerve crush to dissect the specific contribution of bone marrow RAGE expression. We also subjected WT mice to lethal irradiation and performed reconstitution with bone marrow expressing or devoid of RAGE.

RESEARCH DESIGN AND METHODS

Animals. Eight-week-old male C57/BL6 WT mice (Jackson Laboratories, Bar Harbor, ME) and homozygous RAGE-null mice were used in the study. All animals were housed in a barrier animal facility with 12-h light cycle and were fed regular chow diet (#2918; Harlan Teklad Diets). Certain mice were rendered diabetic with the intraperitoneal injection of streptozotocin (5 days, 50 mg/kg in citrate buffer, 100 mmol/L, pH 4.5; Sigma). Nondiabetic control mice were injected with an equal volume of vehicle. To determine the diabetes status of the animals, blood glucose was measured 7 days after the first streptozotocin injection and then every third week for the duration of the experiment and before killing using a Freestyle blood glucose meter (Abbott; Almeda, CA). Animals with a blood glucose level >13 mmol/L (260 mg/dL) were considered diabetic and were used for further experiments. Mean body weight, blood glucose levels, and plasma insulin levels (Alpco Diagnostics, Salem, NH) are shown (Supplementary Table 1). All animal procedures were approved by the Columbia University and New York University Institutional Animal Care and Use Committees and were performed in accordance with the National Institute of Health Animal Care Guidelines.

Nerve crush. Two months after the confirmation of the diabetes status, animals were subjected to unilateral sciatic nerve crush as described (23,24).

Nerve conduction velocity. Nerve conduction velocity tests were performed as described (2,3) and according to the Diabetes Complications Consortium Nerve Conduction protocol (www.diacomp.org). Mice were intraperitoneally anesthetized with ketamine/xylazine. Body temperature was monitored with a dermal probe and maintained at 37°C with a heating lamp/water heating pad, and skin temperature was maintained at 34°C. A Nicolet Viking II computerized electromyography system was used to stimulate and record all studies (Nicolet Biomedical, Madison, WI).

Myelin fiber density, axonal caliber, and endoneurial vessels quantification. Intact and lesioned sciatic nerves were collected 21 days after surgery. After tissue preparation, embedding, and cutting, cross-sections were prepared and stained with toluidine blue. The myelinated fiber density,

From the [1]Diabetes Research Program, Department of Medicine, New York University Langone Medical Center, New York, New York; the [2]Department of Science, Borough of Manhattan Community College–City University of New York, New York, New York; and the [3]Department of Neurology, Columbia University Medical Center, New York, New York.

Corresponding author: Ann Marie Schmidt, annmarie.schmidt@nyumc.org, or Judyta Juranek, judyta.juranek@nyumc.org.

Received 16 May 2012 and accepted 1 September 2012.

DOI: 10.2337/db12-0632

This article contains Supplementary Data online at http://diabetes.diabetesjournals.org/lookup/suppl/doi:10.2337/db12-0632/-/DC1.

axonal caliber, and endoneurial vessels quantification was performed using NIH ImageJ 7.1 with Cell Counter plug-in. Two full-size cross-sections of distal sciatic nerve fascicule from each group were analyzed. Within one cross-section, centrally located regions of interest (ROI), 200 μm^2, were selected for quantification to ensure proper counting methodology, as described (25–29).

RAGE ligand immunohistochemical distribution, macrophage infiltration, and characterization. Sciatic nerve fragments from unlesioned and distal sciatic nerve fragments from the lesioned animals were collected 7 (macrophages) and 21 (RAGE/ligand distribution) days after surgery. Immunohistochemistry was performed using goat anti-human RAGE (1:100; Genetex, Irvine, CA), rabbit anti-HMGB1, anti-carboxymethyl lysine (CML; 1:100; Abcam, Cambridge, MA), anti-Muc1, anti-S100 (1:100; Abcam), and mouse anti-CD31 (Fitzgerald, Acton, MA). Macrophage infiltration (total number of macrophages per ROI) was determined using rat polyclonal F4/80 (1:100; Abcam) and/or rat polyclonal CD68 (1:100; Abcam, Cambridge, MA); macrophage phenotype, proinflammatory M1 markers rabbit anti-CD86 and iNOS (1:100; Abcam), M2 markers rabbit anti-Arg1 and anti-CD163 (1:100; Abcam), and quantification were performed. Oil-Red-O staining was performed on sciatic nerve longitudinal sections (American MasterTech, Lodi, CA) according to the manufacturer's instructions. The area of staining was calculated using ImageJ (30,31). Note that all images related to immunohistochemistry or special stains are reproduced and enlarged in the Supplementary Data.

Bone marrow transplantation. Six-week-old WT mice were irradiated twice in 3- to 4-h intervals with a 600-rad dose from a ^{137}Cs source (JL Shepherd Mark I Irradiator). Approximately 3 h after second irradiation, mice were anesthetized with isoflurane and intraorbitally injected with the bone marrow suspension, which was prepared by flushing the femora and tibiae from WT and RAGE-null mice, resuspended in Hank's balanced salt solution to a final concentration of 5×10^6 cells/mL. One month after the bone marrow transplantation, mice were rendered diabetic or control, and 2 months later they were subjected to unilateral sciatic nerve crush injury.

Macrophage cell cultures: quantitative mRNA PCR analysis of macrophage phenotype in vivo. Bone marrow–derived macrophages (BMDMs) were obtained from 6-week-old WT or RAGE-null mice and exposed to low glucose (5.5 mmol/L D-glucose) or high glucose (25 mmol/L D-glucose), or carboxymethyl lysine (CML) human serum albumin (AGE) (100 μg/mL), a generous gift from Dr. Eric Boulanger, for the last 48 h of the 7-day time course. Total RNA was isolated and quantitative real-time PCR was performed. The primers CD86 (Mm00444543_m1) and Arg1 (Mm00475988_m1) and probe mixture were purchased from Applied Biosystems (Applied Biosystems, Branchburg, NJ). Data were calculated by $2^{-\Delta\Delta Ct}$ method (32) and expressed as the fold increase over the indicated controls (designated as 1) in each figure.

Statistical analysis. Statistical analysis was performed using Graphpad InStat (Graphpad, La Jolla, CA). All values are presented as mean ± SEM. The statistical significance of differences ($P < 0.05$) was evaluated by one-way ANOVA with Tukey post hoc and followed by two-tailed t test (for within-group comparison).

RESULTS

RAGE deficiency facilitates axonal regeneration in the acutely injured diabetic nerve: pathological and functional studies. We probed the effects of global RAGE deficiency in mice subjected to acute sciatic nerve injury. Morphological analysis of unlesioned nerves revealed no significant differences (Fig. 1*A–E*). Twenty-one days postcrush at the site distal to injury, the number of myelinated fibers per mm^2 was reduced by nearly 50% compared with baseline, and a significant difference between WT nondiabetic and diabetic mice was observed (Fig. 1*E* and *J*; $P < 0.05$). Compared with diabetic WT mice postcrush, diabetic RAGE-null mice displayed significantly higher myelinated fiber density (Fig. 1*J*; $P < 0.05$).

To establish the impact of diabetes and RAGE on functional responses to sciatic nerve crush, we assessed motor and sensory conduction velocities. At baseline, motor and sensory nerve conduction velocity studies revealed no significant differences (Fig. 1*K* and *L*). Postcrush, compared with WT nondiabetic mice, diabetic mice displayed significantly lower sensory (Fig. 1*M*; $P < 0.001$) and motor (Fig. 1*N*; $P < 0.05$) conduction velocities. Significantly higher sensory and motor conduction velocities were observed between diabetic WT and diabetic RAGE-null mice Fig. 1*M*, *N*, respectively; $P < 0.05$).

Distribution of RAGE and its ligands after acute injury to the peripheral nerve. We next studied RAGE and RAGE ligand expression 21 days after injury. Prominent RAGE staining was observed in WT nerves (not RAGE-null; not shown). In both nondiabetic and diabetic WT mice, crush injury was associated with a significant increase in RAGE expression (Fig. 2*A–C*; $P < 0.05$ and $P < 0.001$, respectively). RAGE expression in the crushed diabetic nerve was significantly higher than that observed in the crushed nondiabetic nerve (Fig. 2*A–C*; $P < 0.001$). RAGE expression colocalized to perineurial elements (Muc1), blood vessels (CD31), and Schwann cells (S100) in the regenerating nerve (Supplementary Fig. 1).

To determine RAGE ligand distribution, we quantified the number of CML-AGE and HMGB1-positive fibers in control and diabetic nerves at baseline and 21 days postcrush. Immunofluorescence staining revealed significantly higher numbers of immunopositive fibers for HMGB1 and CML-AGE at baseline between WT diabetic compared with nondiabetic nerve (Fig. 2*F–I*, respectively; $P < 0.05$). Compared with WT diabetic mice, RAGE-null diabetic mice displayed significantly lower CML-AGE–expressing fibers at baseline (Fig. 2*G–I*; $P < 0.05$). In all mice tested, HMGB1 and CML-AGE–positive fibers were two-fold to three-fold higher in the postcrushed nerve compared with the uninjured nerve, irrespective of the presence or absence of RAGE or the diabetic state (Fig. 2*D–I*).

Diabetes and RAGE-dependent regeneration in sciatic nerve crush. In parallel with reduced nerve fiber regeneration, diabetes resulted in a significant decrease in endoneurial vessels and regenerating axons at the crush side on day 21 ($P < 0.01$), which was significantly improved by RAGE deletion ($P < 0.05$) (Fig. 3*A–D*). Oil-Red-O staining of nerve segments on day 21 postcrush was significantly lower in diabetic RAGE-null mice compared with WT diabetic mice (Fig. 3*E–H*).

Macrophage infiltration in sciatic nerve tissue postcrush: effect of diabetes and RAGE. These data suggested that Wallerian degeneration and inflammatory mechanisms were impaired in diabetes and restored, at least in part, by RAGE deletion. To further interrogate this hypothesis, we determined macrophage infiltration in the peripheral nerve at three distinct sites (Supplementary Fig. 2) 7 days postsurgery, previously established as an important time point in the postcrush inflammatory response (33) (Fig. 4*A–G*). On the crushed side, in WT mice, diabetes resulted in a significant increase in total number of F4/80-positive macrophages per ROI (Fig. 4*G*; $P < 0.05$). The RAGE-null diabetic crush side displayed a trend toward higher number of F4/80-positive macrophages per ROI compared with the diabetic WT (Fig. 4*G*). In the perineurium, although diabetes did not affect the number of F4/80-positive macrophages per ROI, RAGE-null nondiabetic and RAGE-null diabetic tissue displayed significantly higher F4/80-positive macrophages per ROI compared with their respective WT controls (Fig. 4*G*; $P < 0.001$). At the distal side, in WT mice, diabetes resulted in a significant increase in F4/80-positive macrophages per ROI compared with the nondiabetic condition (Fig. 4*G*; $P < 0.05$). There were significantly higher F4/80-positive macrophages in the ROI in the diabetic compared with the nondiabetic RAGE-null tissue (Fig. 4*G*; $P < 0.05$). At

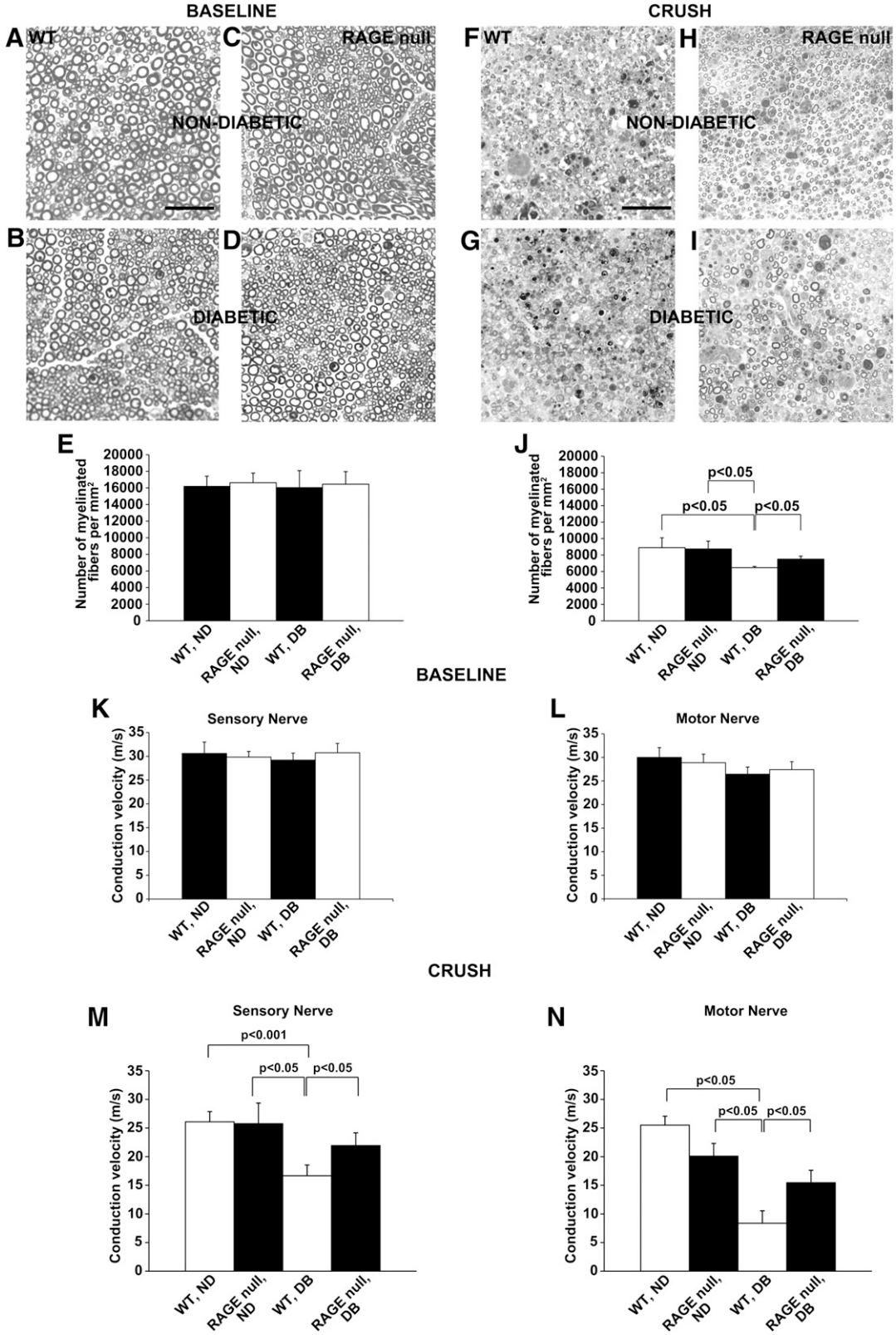

FIG. 1. Deletion of RAGE in diabetic mice restores effective axonal regeneration and improves nerve conduction velocity after acute sciatic nerve crush. Histological analysis shows sciatic nerve myelinated fibers 21 days after acute injury in nondiabetic and diabetic mice. *A–E*: Unlesioned nerve at baseline. *F–J*: Crushed nerve 21 days after surgery. Semithin sections reveal a significant difference in number of myelinated fibers per mm^2 between WT and RAGE-null diabetic mice, indicating that RAGE deletion is beneficial for nerve regeneration in chronic hyperglycemia after injury. Scale bar: 50 μm^2, *n* = 9 mice per group. *K–N*: Nerve conduction velocity (NCV) studies in unlesioned nerve at baseline (*K*, *L*) and acutely injured (*M*, *N*) nerve 21 days postcrush were performed. NCV analysis indicated that although there were no baseline differences, conduction velocity was significantly improved in RAGE-null diabetic mice compared with their WT diabetic counterparts; *n* = 15 mice per group.

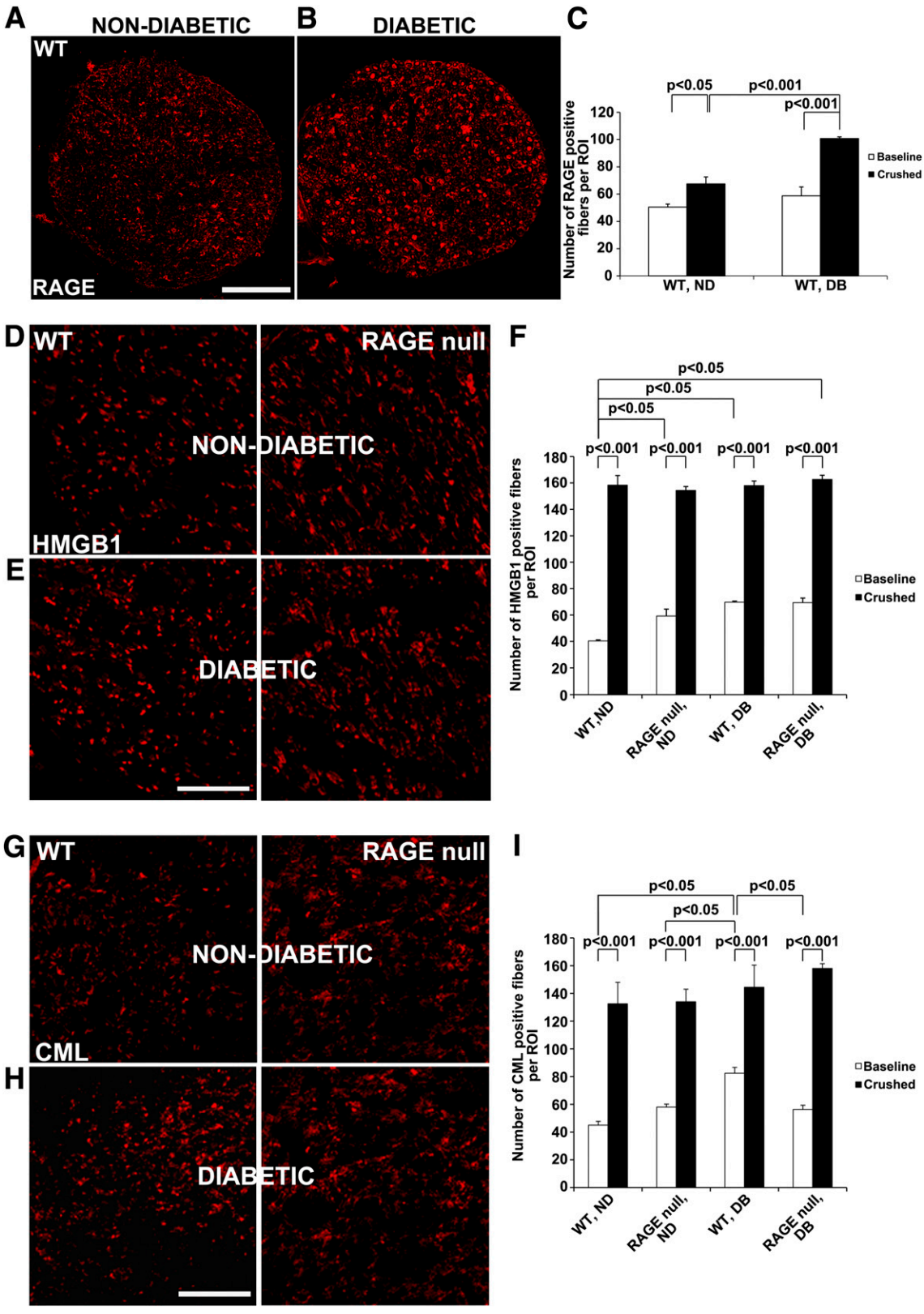

FIG. 2. Expression of RAGE and its ligands in diabetic peripheral nerve: baseline and postcrush injury. The indicated mouse groups were subjected to acute sciatic nerve crush injury and the indicated staining performed in (*A*, *B*, *D*, *E*, *G*, and *H*). *A–C*: RAGE in the sciatic nerve tissue 21 days postcrush injury. *D–F*: HMGB1 in the sciatic nerve tissue 21 days postcrush injury. *G–I*: CML-AGE in the sciatic nerve tissue 21 days postcrush injury. Similar staining was performed at baseline uncrushed state (not shown) and the results were subjected to quantification as illustrated by open bars; filled bars reflect crushed state. Scale bar: 100 μm; *n* = 5 mice per group. (A high-quality digital representation of this figure is available in the online issue.)

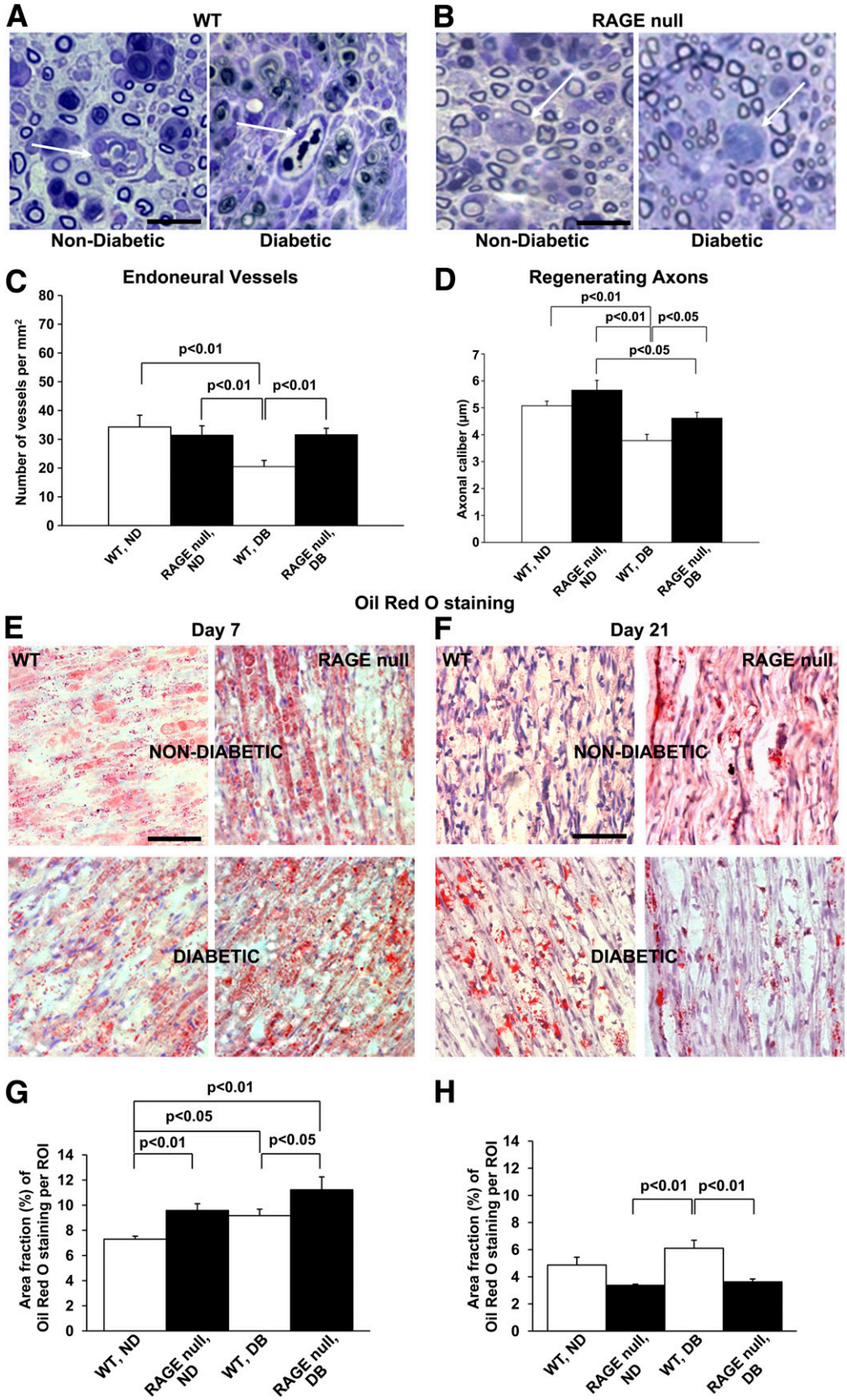

FIG. 3. Morphometric analysis of sciatic nerve regeneration. Number of endoneurial vessels and axonal caliber of regenerating axons were quantified in crushed sciatic nerve section of nondiabetic and diabetic mice 21 days postsurgery (*A–D*). Magnified images show endoneurial vessels (arrows) and size of regenerating axons (*A*, *B*), scale bar 25 μm. The number of vessels was significantly lower in the WT diabetic group as compared with its counterpart, and improved by RAGE deletion in diabetes (*C*). The shortest caliber of regenerating axons was noticed in the diabetic WT group (*D*); *n* = 9 per group. Oil-Red-O staining was performed on longitudinal nerve sections 7 and 21 days postsurgery (*E–H*). On day 7 (*E*, *G*), the most abundant staining was observed for the RAGE-null diabetic group, whereas on day 21 (*F*, *H*) the largest area of staining was observed for WT diabetic group. Scale bar: 50 μm, *n* = 5. (A high-quality digital representation of this figure is available in the online issue.)

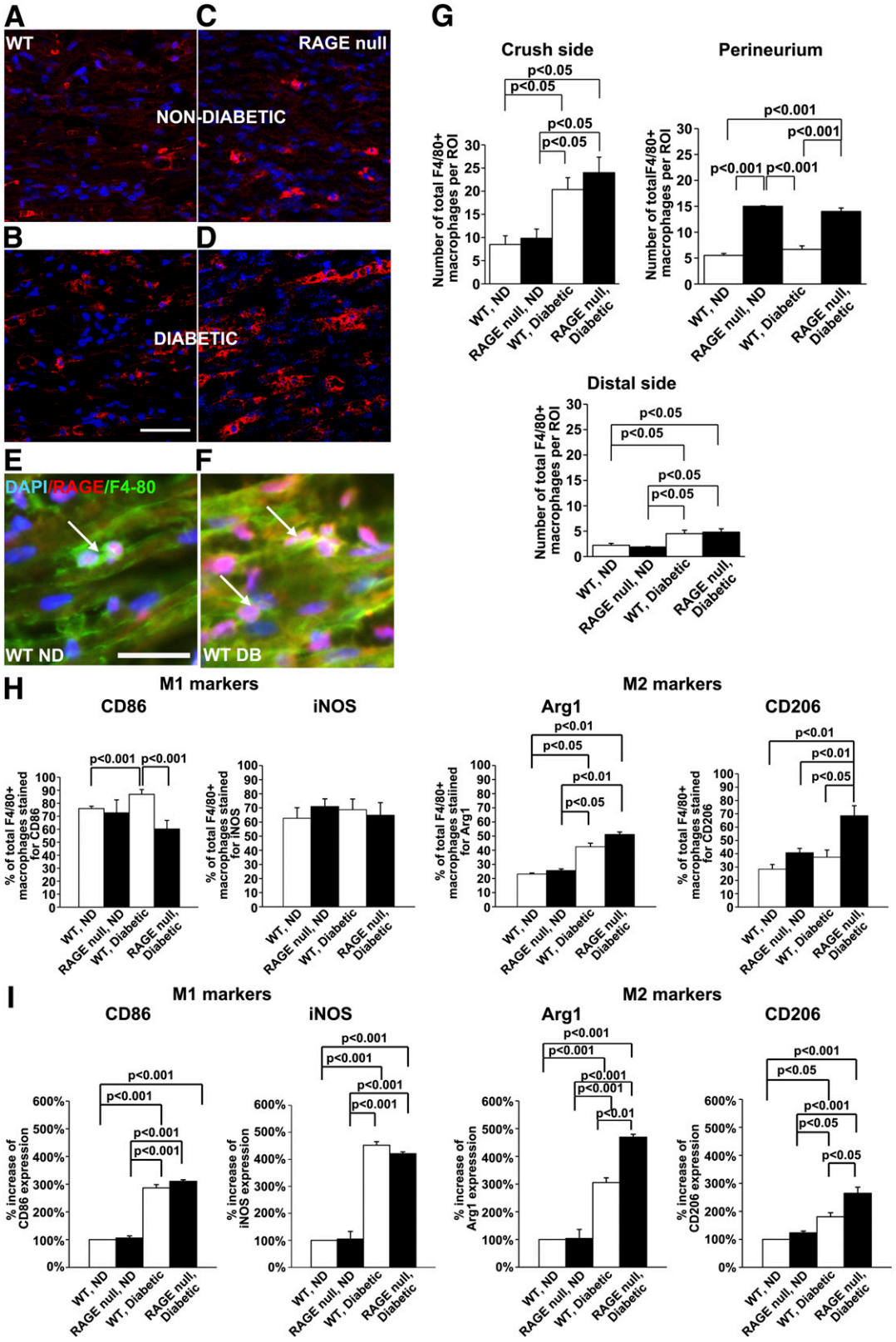

FIG. 4. Macrophage infiltration and polarization in diabetes and crush injury: effect of RAGE. The indicated groups of mice were subjected to diabetes or nondiabetes state; on day 7 after injury, tissue was retrieved and the indicated immunostaining experiments were performed as follows. *A–D*: Immunofluorescence staining for F4/80 (red) and DAPI (nuclei) staining of sciatic nerve cross-section in the indicated mouse groups 7 days after injury. Scale bar: 50 μm. *E* and *F*: Representative images of sciatic nerve cross-sections multistained for RAGE (red) and F4/80 (green) and DAPI (blue). Scale bar 25 μm. *G*: Statistical analysis of macrophage infiltration at three different sections of the nerve. Results are reported as total macrophage number per ROI as determined by F4/80 staining. *H* and *I*: Invading macrophages were stained for M1 and M2 markers (M1, CD86, and iNOS) and (M2, Arg1, and CD206). *H*: Results are depicted as the percent of total macrophages costained for individual markers. *I*: Results for M1 and M2 markers are depicted by setting the WT nondiabetic condition as 100% for reference and all other groups compared with this condition; *n* = 6 mice per condition. (A high-quality digital representation of this figure is available in the online issue.)

baseline without crush, there were no significant differences in macrophage numbers in sciatic nerve tissue among all groups (Supplementary Fig. 3).

M1- and M2-inflammatory macrophage polarization: the impact of diabetes and RAGE. We next quantified the expression of prototypical M1 compared with M2 markers after crush because in general, these markers are associated with proinflammatory compared with reparative signatures, respectively (34,35). Nerve tissue distal to the site of crush was stained for F4/80 and M1 and M2 macrophage markers, and the data were analyzed by assessing the percentage of F4/80-positive macrophages (total macrophage number) double-stained for respective markers per ROI in each experimental condition. In this way, we were able to account for differences in total numbers of macrophages per condition. We tested CD86 and iNOS as prototypical M1 markers and Arg1 and CD206 as prototypical M2 markers. The percentage of $CD86^+$ macrophages was significantly higher in diabetic compared with nondiabetic WT mice (Fig. 4*H*; $P < 0.001$); a trend was noted for percentage of macrophages staining positively for iNOS in WT diabetic vs. nondiabetic mice (Fig. 4*H*). In diabetic RAGE-null mice, the percentage of $CD86^+$ macrophages was significantly lower than that observed in the diabetic WT (Fig. 4*H*; $P < 0.001$). Similar trends were noted for $iNOS^+$ macrophages. There were no differences between WT compared with RAGE-null percentage of $CD86^+$ macrophages, or $iNOS^+$ macrophages in the nondiabetic groups (Fig. 4*H*).

Analysis of M2 markers revealed a different pattern. There was a significant increase in percentage of $Arg1^+$ macrophages in diabetic compared with nondiabetic WT mice (Fig. 4*H*; $P < 0.05$). However, in diabetic RAGE-null mice, a trend toward higher percentage of $Arg1^+$ macrophages was observed compared with the WT diabetic mice (Fig. 4*H*). In the nondiabetic state, there were no differences in Arg1 between WT and RAGE-null mice (Fig. 4*H*). In the case of CD206, we found a trend toward increased percentage of $CD206^+$ macrophages in diabetic compared with nondiabetic WT mice (Fig. 4*H*), and a significantly higher percentage of $CD206^+$ macrophages was found in the diabetic RAGE-null compared with the diabetic WT mice (Fig. 4*H*; $P < 0.05$). Taken together, the diabetic RAGE-deficient state was notable for higher percentage of M2 macrophage markers compared with the diabetic WT mice, and reduced percentage of $CD86^+$ M1 markers compared with WT diabetic mice postcrush.

Data were also analyzed by setting the total absolute number of M1- or $M2^+$-expressing cells in the WT nondiabetic state as 100%; similar results and conclusions were obtained (Fig. 4*I*).

Effect of bone marrow RAGE expression on the response to nerve crush: pathological and functional studies. To test the specific role of bone marrow RAGE expression, we subjected WT mice to lethal irradiation and reconstitution with RAGE-null or WT bone marrow. Four weeks after bone marrow transplantation, mice were rendered diabetic or control, and nerve crush was performed 2 months later. There were no differences in myelinated fiber density at baseline (Fig. 5*A–E*). However, diabetes resulted in significantly lower myelinated fiber density in WT recipients of WT bone marrow postcrush (Fig. 5*F–J*; $P < 0.05$). A statistically significantly higher number of myelinated fibers was observed between RAGE-null compared with WT donor bone marrow in WT diabetic recipient mice postcrush (Fig. 5*F–J*; $P < 0.05$); no significant differences were observed in the nondiabetic state between RAGE-expressing compared with RAGE-null bone marrow (Fig. 5*F–J*).

No baseline differences in sensory or motor conduction velocities were observed between recipients of WT or RAGE-null bone marrow in the nondiabetic or diabetic states (Fig. 5*K* and *L*). 21 days postcrush, in the diabetic state, WT mice reconstituted with WT bone marrow revealed a significant reduction in both sensory and motor conduction velocities (Fig. 5*M*, $P < 0.05$; and Fig. 5*N*, $P < 0.001$). Whereas there were no differences between conduction velocities in WT recipients of WT compared with RAGE-null bone marrow in the nondiabetic state, there was a trend toward higher sensory nerve conduction velocity in diabetic RAGE-null mice compared with diabetic WT mice (Fig. 5*M*) and a statistically significant increase in motor conduction velocity in WT diabetic recipients receiving RAGE-null compared with WT bone marrow (Fig. 5*N*; $P < 0.05$).

Macrophage infiltration in sciatic nerve tissue postcrush: effect of RAGE expression in bone marrow. We then probed the effect of RAGE expression in the bone marrow on macrophage infiltration postcrush (Fig. 6*A–E*). Whereas in the nondiabetic state there was no effect of bone marrow RAGE expression on the numbers of F4/80-positive cells per ROI on the crush side (Fig. 6*E*, left), a significantly higher number of F4/80-positive macrophages was observed in WT nondiabetic recipients of RAGE-null compared with WT bone marrow in the perineurium (Fig. 6*E*, right; $P < 0.01$). In the diabetic state, on both the crush side and the perineurium, diabetic recipients of RAGE-null compared with WT bone marrow displayed significantly higher numbers of macrophages (Fig. 6*E*, left and right; $P < 0.01$ and $P < 0.05$, respectively). At baseline without crush, there were no significant differences in macrophages in sciatic nerve tissue among all groups (Supplementary Fig. 4).

Next, we tested the percentage of F4/80-positive macrophages double-stained for M1 markers. The percentage of $CD86^+$ and percentage of $iNOS^+$ macrophages did not differ between diabetic compared with nondiabetic WT recipient mice receiving WT donor bone marrow. The percentage of $CD86^+$ and the percentage of $iNOS^+$ macrophages were significantly higher in WT diabetic recipients receiving RAGE-null compared with WT donor bone marrow (Fig. 6*F*; $P < 0.05$).

Next, we assessed M2 markers. In diabetes, there was a significant increase in percentage of $Arg1^+$ and percentage of $CD206^+$ macrophages per total macrophages in WT compared with nondiabetic mice receiving WT bone marrow (Fig. 6*F*; $P < 0.01$ and $P < 0.05$, respectively). We found that there was a significantly higher percentage of $Arg1^+$ macrophages per total number of macrophages in diabetic WT recipient mice receiving RAGE-null compared with WT bone marrow (Fig. 6*F*; $P < 0.001$), and a trend toward increased percentage of $CD206^+$ macrophages in diabetic mice receiving RAGE-null compared with WT bone marrow. In the nondiabetic recipients of RAGE-null compared with WT bone marrow, significantly higher percentage of Arg1 and $CD206^+$ macrophages were found in the WT nondiabetic recipients of RAGE-null compared with WT bone marrow (Fig. 6*F*; $P < 0.01$ and $P < 0.05$, respectively). Analogous findings were found when the data were analyzed by arbitrarily setting as 100% the number of macrophages per total macrophages in the WT nondiabetic groups (Fig. 6*G*).

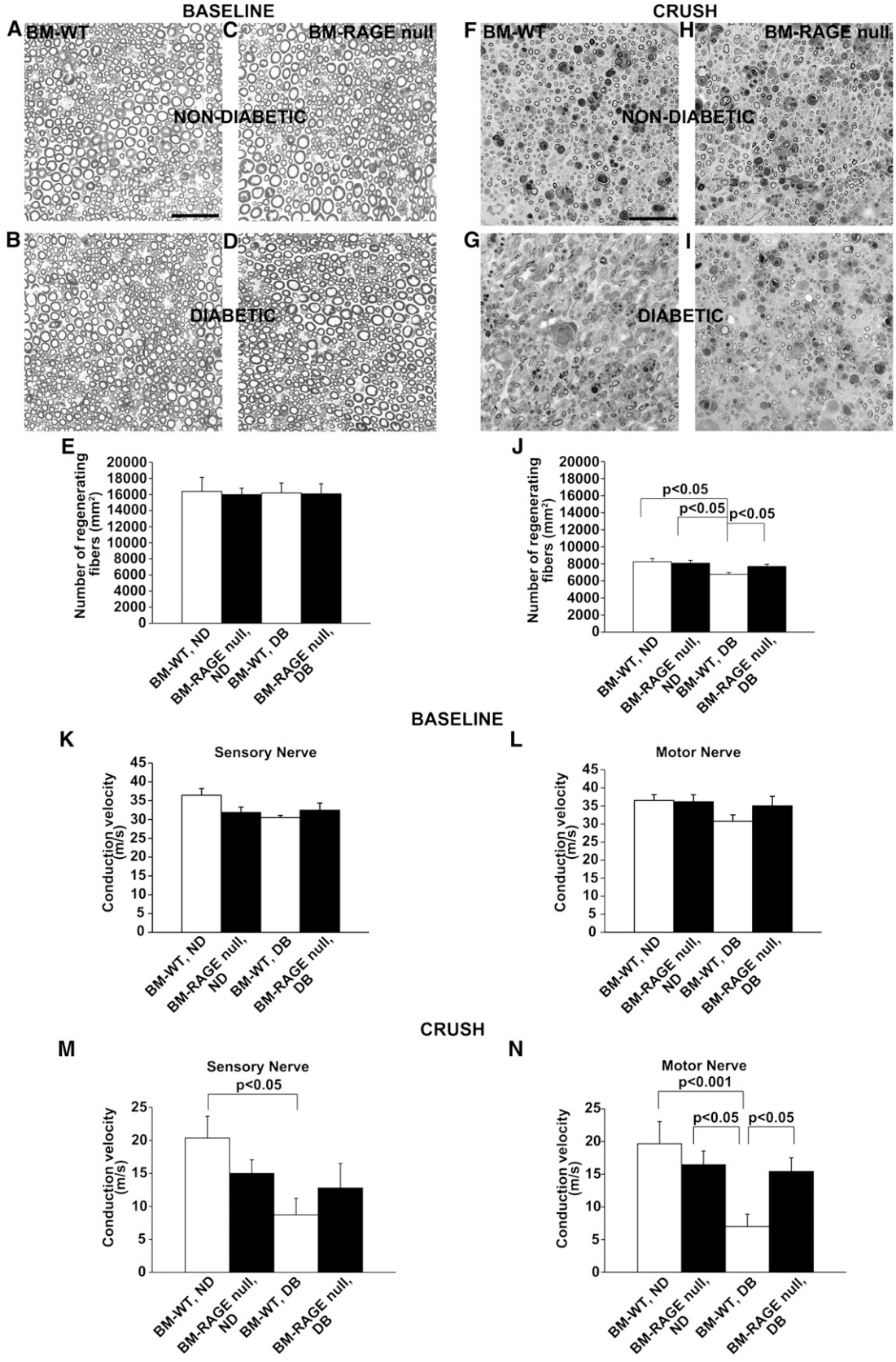

FIG. 5. Deletion of RAGE in bone marrow in diabetic mice restores effective axonal regeneration and improves conduction velocity after acute sciatic nerve crush. Histological analysis of sciatic nerve myelinated fibers 21 days after acute injury in WT mice subjected to lethal irradiation and reconstitution with the indicated bone marrow (WT or RAGE-null) followed 4 weeks later by induction of diabetes or nondiabetic state. *A–E*: Unlesioned nerve at baseline. *F–J*: Crushed nerve 21 days postsurgery. Semithin sections reveal a significant difference in number of myelinated fibers per mm^2 between WT mice reconstituted with RAGE-null compared with WT bone marrow in the diabetic state, indicating that transplantation of RAGE-deficient bone marrow is beneficial for nerve regeneration in diabetes after injury. Scale bar: 50 μm, *n* = 8 mice per group.

Taken together, the absence of RAGE expression in the bone marrow, particularly in the diabetic state, was sufficient to restore myelinated fiber density and conduction velocity, in parallel with significantly increased M2 polarization markers of macrophages in the nerve tissue postcrush.

BMDMs and polarization: effect of AGE-RAGE. To study macrophage polarization in vitro, we incubated BMDMs in low (5.5 mmol/L D-glucose) compared with high diabetes-relevant (25 mmol/L D-glucose) conditions, or CML–human serum albumin (HSA) AGE. As shown in Fig. 7*A*, incubation of WT BMDMs with high glucose for 7 days resulted in a trend to increased CD86 mRNA transcripts, and incubation of WT BMDMs with CML-HSA AGE for 48 h resulted in a highly significant increase in CD86 mRNA transcripts ($P < 0.001$). Consistent with roles for RAGE in regulation of CD86 by AGEs, incubation of RAGE-null BMDMs with CML-HSA resulted in significantly lower CD86 mRNA transcripts compared with wild-type BMDMs (Fig. 7*B*; $P < 0.001$). There were no differences between CD86 mRNA transcripts observed in WT BMDMs compared with RAGE-null BMDMs grown in high glucose, at least during this time course.

In the case of M2 markers, incubation of WT BMDMs with CML-HSA AGE or with high glucose for 7 days resulted in highly significant downregulation of Arg1 mRNA transcripts (Fig. 7*C*; $P < 0.001$). Key roles for RAGE were identified; incubation of RAGE-null BMDMs with CML-HSA AGE resulted in significantly higher Arg1 mRNA transcripts compared with WT BMDMs (Fig. 7*D*; $P < 0.05$). There were no significant effects of RAGE expression in high-glucose-treated BMDMs (Fig. 7*D*) during this time course.

DISCUSSION

Our previous studies illustrated that deletion of RAGE was protective in murine models of long-term diabetes-associated neuropathy (14,15). Because RAGE is critically involved in inflammatory mechanisms by virtue of its ability to bind members of the S100/calgranulin family, HMGB1 and Mac-1 (19,20,36), we tested its role in superimposed acute nerve crush injury. These studies bear clinical relevance because diabetic subjects often sustain thermal and other acute injuries to their extremities during advancing neuropathy (7–10). This present work reveals that RAGE, particularly in bone marrow cells and in diabetes, contributes to maladaptive inflammatory mechanisms after acute nerve crush.

Our data confirmed that diabetes was associated with increased expression of AGEs in the peripheral nerve in the basal state (15) and buttressed our findings that AGE levels were lower in diabetic RAGE-null mice compared with diabetic WT mice (37). We previously showed that RAGE suppresses mRNA and protein levels of glyoxalase-1 in murine kidney cortex in diabetic OVE26 mice (37). Glyoxalase-1 is a chief detoxification mechanism that diverts the AGE precursor, methylglyoxal, from forming long-lived AGEs (38). The finding that diabetic RAGE-null mice displayed lower levels of CML-AGE in the peripheral nerve in the basal state supports a key role for RAGE in suppression of anti-AGE defense mechanisms.

Our data reveal that acute injury to the sciatic nerve dramatically increases levels of CML-AGE, irrespective of the state of glycemia or RAGE expression. Previous work by others suggested potential roles for the myeloperoxidase family of enzymes in generation of this prevalent AGE (39). In parallel, the RAGE ligand HMGB1 also was upregulated by crush in all groups, supporting previous findings that HMGB1 is released by damaged cells (40). It is also possible that heretofore unidentified ligands of RAGE may contribute to the response to nerve crush.

Streptozotocin-treated diabetic mice remained consistently diabetic (blood glucose >260 mg/dL) throughout the course of study. By this method of induction of diabetes, levels of insulin were not drastically reduced by streptozotocin, nor were they dependent on RAGE (Supplementary Table 1). Rather, a relatively milder form of diabetes was induced in which streptozotocin-treated mice did not lose weight and were not ketotic. These findings are quite analogous to our earlier studies in which we used the identical streptozotocin regimen in mice devoid of apolipoprotein E to study atherosclerosis (41). In the current study, although these experimental conditions may underlie the lack of significant reduction of nerve conduction velocities in the basal precrush state, they nevertheless assured that the animals were not demonstrating weight loss or ketoacidosis, distinct features that might have confounded data interpretation.

Our data, both in the global state and after bone marrow transplantation, reveal that the effects of RAGE deletion are most striking in diabetes, because deletion of RAGE in nondiabetic mice had no significant beneficial or adverse effect on nerve fiber regeneration or restoration of conduction velocities. We previously showed that strategies to decoy RAGE ligands, via administration of soluble RAGE or introduction of a cytoplasmic tail-deleted mutant of RAGE in peripheral neurons or mononuclear phagocytes, reduced the regenerative response in nondiabetic mice after acute sciatic nerve crush (23,24). Those data suggest that ligands that may act through distinct non-RAGE receptors may impart beneficial adaptive responses in the absence of hyperglycemia. It was shown that upregulation of CD36 (a non-RAGE AGE receptor) in macrophages (42), by pioglitazone, promoted peripheral nerve remyelination after crush injury. The authors showed that postpioglitazone CD36 was upregulated in the infiltrating macrophages, suggesting that CD36 contributed to mechanisms that clear the injured nerve tissue of debris and thus lead to a microenvironment ready for remyelination and regeneration (43). Consistent with these concepts, mice devoid of CD36 revealed delays in remyelination and suppressed clearance of myelin by the invading and local macrophages. By day 21 postcrush, our data revealed significantly reduced Oil-Red-O staining in diabetic RAGE-null compared with WT mice. These data suggest that direct blockade of RAGE in the diabetic nerve is likely to be adaptive, because ligands that might interact with distinct non-RAGE receptors will not be detoured from their regeneration-stimulating targets.

***K–N*: Nerve conduction velocity (NCV) in unlesioned nerve at baseline (*K*, *L*) and acutely injured (*M*, *N*) nerve 21 days postsciatic nerve crush. NCV analysis 21 days postcrush indicated that conduction velocity is significantly improved in WT diabetic mice reconstituted with RAGE-null compared with WT bone marrow; *n* = 15 mice per group.**

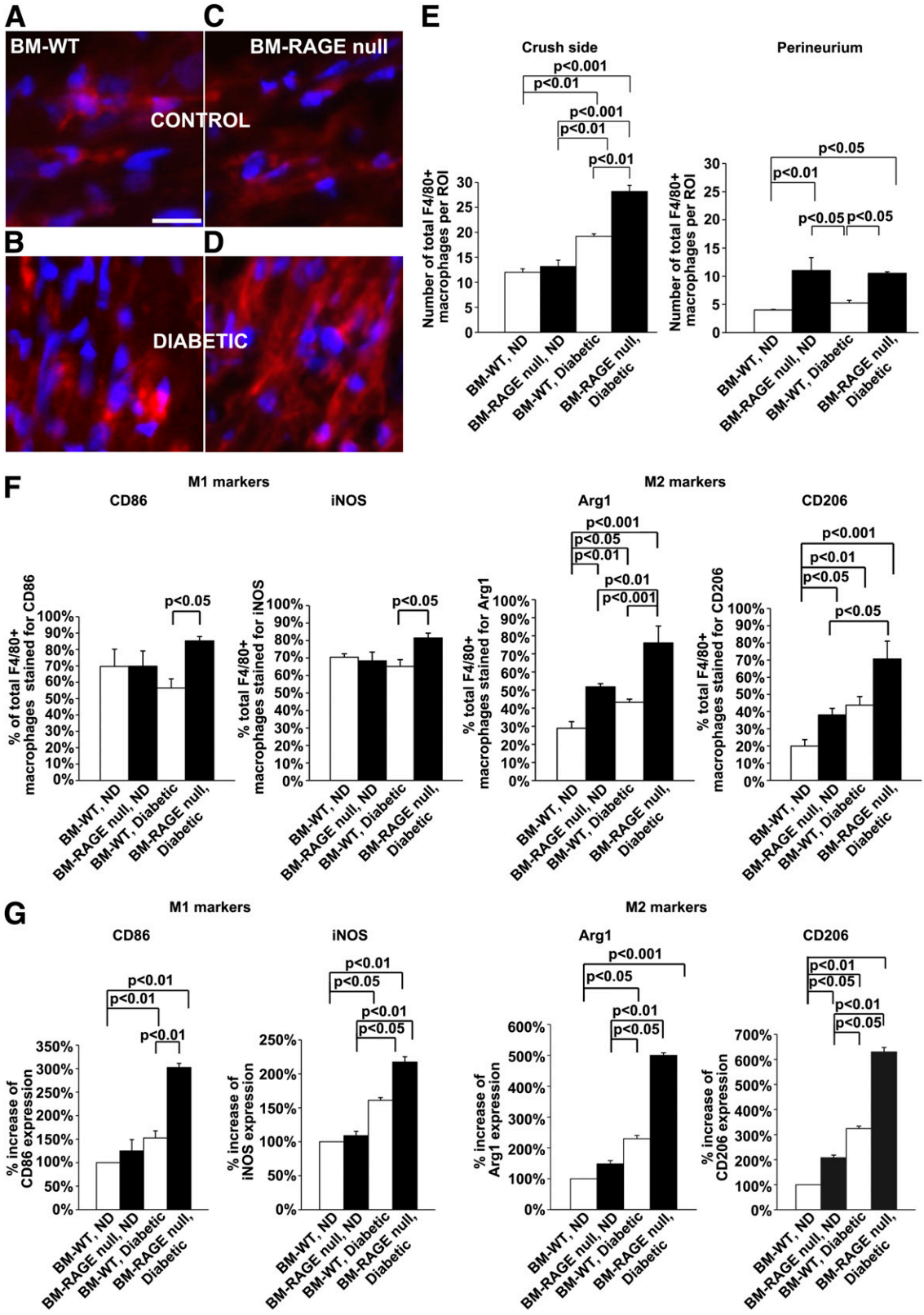

FIG. 6. Macrophage infiltration and polarization in diabetes and crush injury: effect of bone marrow RAGE expression. The indicated groups of mice were subjected to diabetes or nondiabetes state; on day 7 after injury, tissue was retrieved and the indicated immunostaining experiments were performed as follows. *A–D*: Immunofluorescence staining for F4/80 (red) and DAPI (nuclei) staining of sciatic nerve cross-section in the indicated mouse groups 7 days after injury. Scale bar: 25 μm. *E*: Statistical analysis of macrophage infiltration at two different sections of the nerve. Results are reported as total macrophage number per ROI as determined by F4/80 staining. *F*: Invading macrophages were stained for M1 and M2 markers (M1, CD86, and iNOS) and (M2, Arg1, and CD206). Results are depicted as the percent of total macrophages costained for individual markers. *G*: Results are depicted by setting the WT nondiabetic condition as 100% for reference and all other groups compared with this condition; *n* = 6 mice per condition. (A high-quality digital representation of this figure is available in the online issue.)

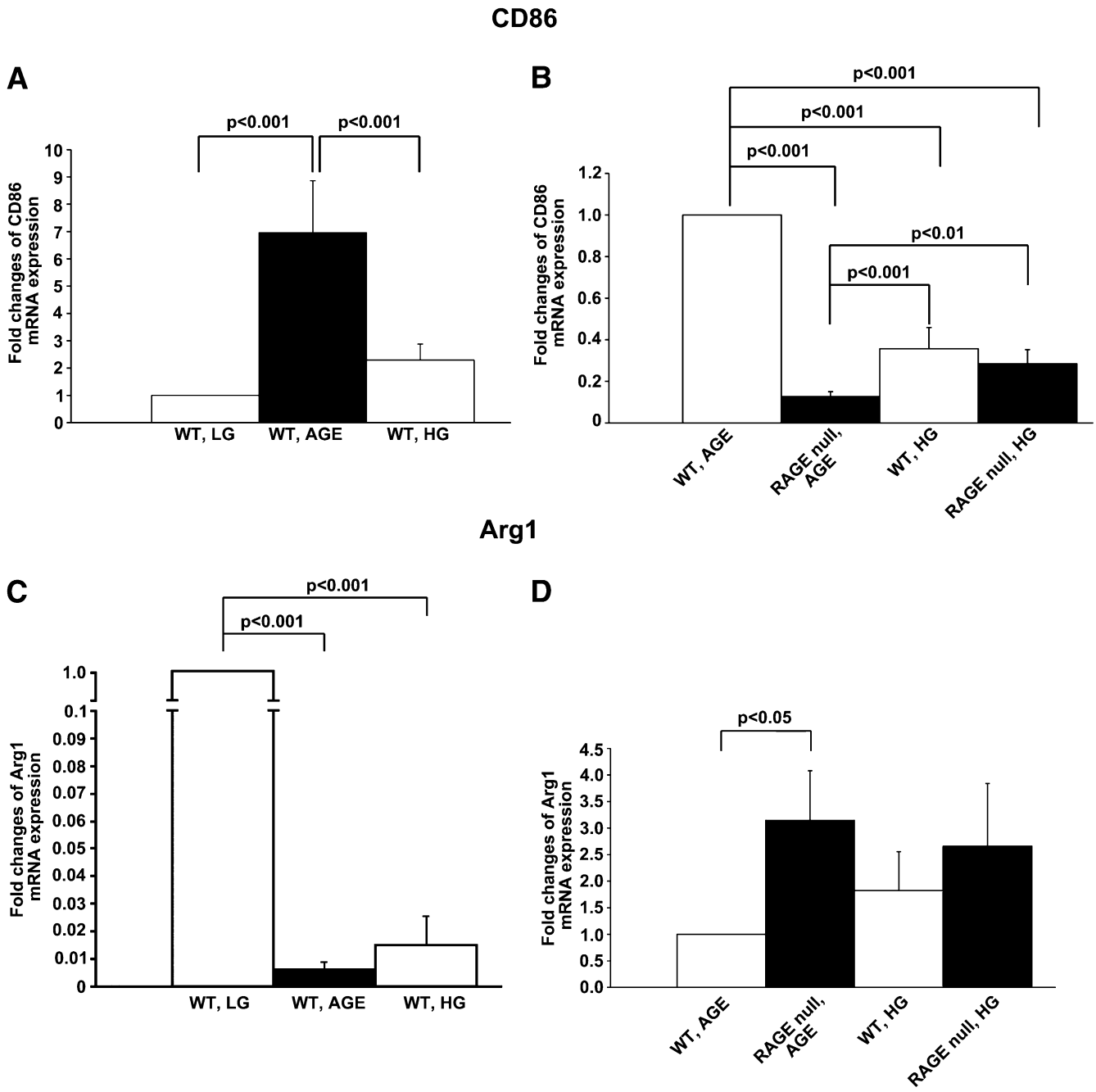

FIG. 7. RAGE modulates macrophage polarization in BMDMs: effect of glucose and AGE. BMDMs were retrieved from the indicated mice and incubated for 7 days with low physiologic levels of glucose (5.5 mmol/L D-glucose) or high glucose (diabetes-relevant) (25 mmol/L D-glucose). In other studies, BMDMs were incubated in physiologic levels of glucose (5.5 mmol/L D-glucose) and CML-HSA (100 μg/mL) for 48 h. Macrophages were retrieved and subjected to real-time quantitative PCR. *A* and *C*: The effects of glucose and AGEs on WT BMDM expression of CD86 and Arg1 (respectively) are shown. WT low-glucose incubated BMDMs were set as reference. *B* and *D*: The effects of RAGE deletion on glucose and CML-HSA treatment on expression of CD86 and Arg1 (respectively) are shown. WT macrophages exposed to AGE (CML-HSA) are set as the reference. This experiment was repeated for a total of three independent experiments.

We were intrigued by the finding that, in general, RAGE-null nerve tissue postcrush displayed either significantly higher numbers of macrophages (perineurium) or no reduction in the numbers of macrophages (crush and distal sites) compared with the respective RAGE-expressing groups. These findings, together with the demonstrated benefit of deletion of RAGE in the bone marrow, led us to query whether the properties of the macrophages differed by glycemia or RAGE expression status. Although certainly a complex area of biology, it is known that discrete classes of macrophages contribute to a greater degree to active inflammation mechanisms (M1), whereas others play more pronounced roles in repair and regeneration (M2). Individual macrophages may express both M1 and M2 markers; hence, it may be the "balance" of expression of these markers that facilitates sustained inflammation or upregulation of repair and resolution mediators. In global RAGE-null mice and in WT mice reconstituted with RAGE-deficient bone marrow and subjected to nerve crush, particularly in the diabetic state, a consistent finding was that

deletion of RAGE resulted in higher expression of M2 markers, Arg1, and CD206. In the nondiabetic state, deletion of bone marrow RAGE in WT mice also increased Arg1 M2 marker. There was no consistent pattern of RAGE expression with M1 marker expression, suggesting that the principal benefits of RAGE deletion in nerve regeneration were not accounted for in significant measure by changes in M1 macrophage markers. Our studies in isolated BMDMs confirmed that deletion of RAGE in CML-AGE–treated macrophages resulted in higher expression of Arg1 compared with corresponding WT macrophages under the same conditions. Consistent with this concept, diabetic RAGE-null mice postcrush exhibited increased numbers of endoneurial vessels and regenerating axons and reduced Oil-Red-O staining by day 21, all features linked to repair and regeneration.

Previous studies by Kennedy and Zochodne showed that macrophage responses in diabetic peripheral nerve after superimposed crush in rats were impaired; those authors speculated that reduced macrophage function might contribute to impaired Wallerian degeneration, a prerequisite to effective axonal regeneration (13). Terada et al. (44) tested these concepts in a murine model of diabetes and sciatic nerve transection. They showed that Wallerian degeneration was significantly delayed in the diabetic compared with the nondiabetic nerve, but the mechanisms by which macrophage properties were impacted were not studied (44). Nevertheless, these previous studies suggested that peripheral nerve regeneration in diabetic mice with superimposed acute nerve damage was impaired, at least in part via delayed and less effective Wallerian degeneration, a process that requires effective macrophage function and a balance between proinflammatory and tissue-restorative activities. Our data provide a mechanistic explanation for these findings. We may deduce that M1 macrophage responses in the injured nerve segments must be counterbalanced by reparative M2 responses to facilitate clearance of myelin debris with the generation of an environment conducive for nerve fiber regeneration.

Recently, Parathath et al. (45) showed that in hyperlipidemic, atherosclerosis-vulnerable mice, diabetes slowed regression of atherosclerosis. The authors noted that diabetes skewed macrophage polarization toward the M1 compared with the M2 phenotype (45) and that lesional collagen content, usually linked to plaque stability and less inflammation, was reduced in the diabetic plaques. Because collagen formation is typically associated with M2 polarization (46), these data suggest that M1 macrophage polarization may have contributed, at least in part, to sustained proinflammatory forces and reduced regression.

In conclusion, our data reveal that RAGE-dependent reduction in M2 polarization in the diabetic peripheral nerve after acute nerve crush, at least in part by bone marrow-derived RAGE-expressing cells, is linked to impaired axonal regeneration and reduced recovery of conduction velocities. We show that RAGE may contribute to altered polarization and that global or selective bone marrow deletion of RAGE in diabetes enhances M2 macrophage polarization and nerve regeneration consequent to acute injury.

Finally, these data are consistent with our recent work showing quite diverse roles for Myd88 compared with RAGE in survival and regeneration responses in massive liver injury (22). We conclude that RAGE is not critical for innate repair responses in the acutely injured diabetic nerve, and surmise that blocking the chronic maladaptive effects of inflammatory cell RAGE signaling in this setting may contribute to prevention of long-term damage and to the mediation of effective acute responses to injury via restoration of adaptive macrophage responses.

ACKNOWLEDGMENTS

A.M.S. received funding for this research from the US Public Health Service (AG17490).

No potential conflicts of interest relevant to this article were reported.

J.K.J. co-designed the experiments. J.K.J. performed research. J.K.J., M.S.G., and T.H.B. analyzed the data. J.K.J. wrote the manuscript. M.S.G. contributed to experimental design. M.S.G., F.S., J.Z., J.G., R.R., S.F.Y., and T.H.B. reviewed the manuscript. F.S. contributed to the research (bone marrow transplantation). J.Z., J.G., and R.R. helped perform research and contributed to the discussion. S.F.Y. contributed to the experimental design of the research (primers, rtPCR) and analyzed the data (rtPCR results). S.F.Y. and A.M.S. edited the manuscript. T.H.B. contributed to the experimental design of the research (nerve conduction velocity). A.M.S. designed the experiments and contributed to the writing of the manuscript. A.M.S. is the guarantor of this work and, as such, had full access to all of the data in the study and takes responsibility for the integrity of the data and the accuracy of the data analysis.

Parts of this study were presented in abstract form at the 72nd Scientific Sessions of the American Diabetes Association, Philadelphia, Pennsylvania, 8–12 June 2012, the Annual Meetings of the Society for Neuroscience in 2010 (San Diego, California) and 2008 (Washington, DC), and the 9th Congress of the Polish Society of Clinical Neurophysiology in 2010 (Cracow, Poland).

The authors thank Mr. Yu Shan Zou (Department of Endocrinology, New York University Medical Center) and Mr. Pratik Kothary (student intern, Department of Endocrinology, New York University Medical Center) for their technical support and assistance, Ms. Kristy Brown (Department of Pathology, Columbia University Medical Center) for her excellent help with histological section preparation, and Ms. Latoya Woods for assistance with manuscript preparations (Division of Endocrinology, New York University Medical Center).

REFERENCES

1. Shaw JE, Sicree RA, Zimmet PZ. Global estimates of the prevalence of diabetes for 2010 and 2030. Diabetes Res Clin Pract 2010;87:4–14
2. Zimmet P, Alberti KG, Shaw J. Global and societal implications of the diabetes epidemic. Nature 2001;414:782–787
3. Deshpande AD, Harris-Hayes M, Schootman M. Epidemiology of diabetes and diabetes-related complications. Phys Ther 2008;88:1254–1264
4. Candrilli SD, Davis KL, Kan HJ, Lucero MA, Rousculp MD. Prevalence and the associated burden of illness of symptoms of diabetic peripheral neuropathy and diabetic retinopathy. J Diabetes Complications 2007;21:306–314
5. Hall V, Thomsen RW, Henriksen O, Lohse N. Diabetes in Sub Saharan Africa 1999-2011: epidemiology and public health implications. A systematic review. BMC Public Health 2011;11:564
6. Viswanathan V, Kumpatla S. Pattern and causes of amputation in diabetic patients—a multicentric study from India. J Assoc Physicians India 2011; 59:148–151
7. Boulton AJ. What you can't feel can hurt you. J Vasc Surg 2010;52(Suppl): 28S–30S
8. Putz Z, Nadas J, Jermendy G. Severe but preventable foot burn injury in diabetic patients with peripheral neuropathy. Med Sci Monit 2008;14:CS89–CS91

9. Liniger C, Albeanu A, Moody JF, Richez J, Bloise D, Assal JP. The Thermocross: a simple tool for rapid assessment of thermal sensation thresholds. Diabetes Res Clin Pract 1991;12:25–33
10. Dijkstra S, vd Bent MJ, vd Brand HJ, et al. Diabetic patients with foot burns. Diabet Med 1997;14:1080–1083
11. Polydefkis M, Hauer P, Sheth S, Sirdofsky M, Griffin JW, McArthur JC. The time course of epidermal nerve fibre regeneration: studies in normal controls and in people with diabetes, with and without neuropathy. Brain 2004;127:1606–1615
12. Ebenezer GJ, O'Donnell R, Hauer P, Cimino NP, McArthur JC, Polydefkis M. Impaired neurovascular repair in subjects with diabetes following experimental intracutaneous axotomy. Brain 2011;134:1853–1863
13. Kennedy JM, Zochodne DW. The regenerative deficit of peripheral nerves in experimental diabetes: its extent, timing and possible mechanisms. Brain 2000;123:2118–2129
14. Bierhaus A, Haslbeck K-M, Humpert PM, et al. Loss of pain perception in diabetes is dependent on a receptor of the immunoglobulin superfamily. J Clin Invest 2004;114:1741–1751
15. Toth C, Rong LL, Yang C, et al. Receptor for advanced glycation end products (RAGEs) and experimental diabetic neuropathy. Diabetes 2008; 57:1002–1017
16. Yan SF, Ramasamy R, Schmidt AM. Mechanisms of disease: advanced glycation endproducts and their receptor in inflammation and diabetes complications. Nat Rev Endocrinol 2008;4:285–293
17. Barlovic DP, Soro-Paavonen A, Jandeleit-Dahm KA. RAGE biology, atherosclerosis and diabetes. Clin Sci (Lond) 2011;121:43–55
18. Yan SF, Ramasamy R, Schmidt AM. Receptor for AGE (RAGE) and its ligands-cast into leading roles in diabetes and the inflammatory response. J Mol Med (Berl) 2009;87:235–247
19. Hofmann MA, Drury S, Fu C, et al. RAGE mediates a novel proinflammatory axis: a central cell surface receptor for S100/calgranulin polypeptides. Cell 1999;97:889–901
20. Taguchi A, Blood DC, del Toro G, et al. Blockade of RAGE-amphoterin signalling suppresses tumour growth and metastases. Nature 2000;405: 354–360
21. Cataldegirmen G, Zeng S, Feirt N, et al. RAGE limits regeneration after massive liver injury by coordinated suppression of TNF-alpha and NF-kappaB. J Exp Med 2005;201:473–484
22. Zeng S, Zhang QY, Huang J, et al. Opposing roles of RAGE and Myd88 signaling in extensive liver resection. FASEB J 2012;26:882–893
23. Rong LL, Yan SF, Wendt T, et al. RAGE modulates peripheral nerve regeneration via recruitment of both inflammatory and axonal outgrowth pathways. FASEB J 2004;18:1818–1825
24. Rong LL, Trojaborg W, Qu W, et al. Antagonism of RAGE suppresses peripheral nerve regeneration. FASEB J 2004;18:1812–1817
25. Fazan VP, Salgado HC, Barreira AA. A descriptive and quantitative light and electron microscopy study of the aortic depressor nerve in normotensive rats. Hypertension 1997;30:693–698
26. Hunter DA, Moradzadeh A, Whitlock EL, et al. Binary imaging analysis for comprehensive quantitative histomorphometry of peripheral nerve. J Neurosci Methods 2007;166:116–124
27. Mayhew TM, Sharma AK. Sampling schemes for estimating nerve fibre size. I. Methods for nerve trunks of mixed fascicularity. J Anat 1984;139: 45–58
28. Said G, Lacroix C, Lozeron P, Ropert A, Planté V, Adams D. Inflammatory vasculopathy in multifocal diabetic neuropathy. Brain 2003;126:376–385
29. Shan X, Chiang PM, Price DL, Wong PC. Altered distributions of Gemini of coiled bodies and mitochondria in motor neurons of TDP-43 transgenic mice. Proc Natl Acad Sci USA 2010;107:16325–16330
30. Narasimhan SD, Yen K, Bansal A, Kwon ES, Padmanabhan S, Tissenbaum HA. PDP-1 links the TGF-β and IIS pathways to regulate longevity, development, and metabolism. PLoS Genet 2011;7:e1001377
31. Gerrits MF, Ghosh S, Kavaslar N, et al. Distinct skeletal muscle fiber characteristics and gene expression in diet-sensitive versus diet-resistant obesity. J Lipid Res 2010;51:2394–2404
32. Livak KJ, Schmittgen TD. Analysis of relative gene expression data using real-time quantitative PCR and the 2(-Δ Δ C(T)) Method. Methods 2001;25: 402–408
33. Fu SY, Gordon T. The cellular and molecular basis of peripheral nerve regeneration. Mol Neurobiol 1997;14:67–116
34. Lawrence T, Natoli G. Transcriptional regulation of macrophage polarization: enabling diversity with identity. Nat Rev Immunol 2011;11:750–761
35. Geissmann F, Gordon S, Hume DA, Mowat AM, Randolph GJ. Unravelling mononuclear phagocyte heterogeneity. Nat Rev Immunol 2010;10:453–460
36. Chavakis T, Bierhaus A, Al-Fakhri N, et al. The pattern recognition receptor (RAGE) is a counterreceptor for leukocyte integrins: a novel pathway for inflammatory cell recruitment. J Exp Med 2003;198:1507–1515
37. Reiniger N, Lau K, McCalla D, et al. Deletion of the receptor for advanced glycation end products reduces glomerulosclerosis and preserves renal function in the diabetic OVE26 mouse. Diabetes 2010;59:2043–2054
38. Thornalley PJ. Glyoxalase I—structure, function and a critical role in the enzymatic defence against glycation. Biochem Soc Trans 2003;31:1343–1348
39. Anderson MM, Requena JR, Crowley JR, Thorpe SR, Heinecke JW. The myeloperoxidase system of human phagocytes generates Nepsilon-(carboxymethyl)lysine on proteins: a mechanism for producing advanced glycation end products at sites of inflammation. J Clin Invest 1999;104:103–113
40. Scaffidi P, Misteli T, Bianchi ME. Release of chromatin protein HMGB1 by necrotic cells triggers inflammation. Nature 2002;418:191–195
41. Park L, Raman KG, Lee KJ, et al. Suppression of accelerated diabetic atherosclerosis by soluble receptor for advanced glycation endproducts. Nat Med 1998;4:1025–1031
42. Ohgami N, Nagai R, Ikemoto M, et al. Cd36, a member of the class b scavenger receptor family, as a receptor for advanced glycation end products. J Biol Chem 2001;276:3195–3202
43. Eto M, Sumi H, Fujimura H, Yoshikawa H, Sakoda S. Pioglitazone promotes peripheral nerve remyelination after crush injury through CD36 upregulation. J Peripher Nerv Syst 2008;13:242–248
44. Terada M, Yasuda H, Kikkawa R. Delayed Wallerian degeneration and increased neurofilament phosphorylation in sciatic nerves of rats with streptozocin-induced diabetes. J Neurol Sci 1998;155:23–30
45. Parathath S, Grauer L, Huang LS, et al. Diabetes adversely affects macrophages during atherosclerotic plaque regression in mice. Diabetes 2011; 60:1759–1769
46. O'Brien J, Lyons T, Monks J, et al. Alternatively activated macrophages and collagen remodeling characterize the postpartum involuting mammary gland across species. Am J Pathol 2010;176:1241–1255